CSIS Discussion Paper No. 33

# Analysis of Surface Changes by Tessellations

Yukio Sadahiro

NOVEMBER, 2000

Center for Spatial Information Science
University of Tokyo
7-3-1, Bunkyo-ku, Tokyo 113-8656, Japan

November 21, 2000

# Analysis of Surface Changes by Tessellations


Yukio Sadahiro

Center for Spatial Information Science and Department of Urban Engineering
University of Tokyo
7-3-1, Hongo, Bunkyo-ku, Tokyo 113-8656, Japan

Phone: +81-3-5841-6273
Fax: +81-3-5841-8521
E-mail: sada@okabe.t.u-tokyo.ac.jp

**Analysis of Surface Changes by Tessellations**


**Abstract**

This paper develops a method for analyzing the change of surface, a continuous function defined over the two-dimensional space. The surface change is represented by a scalar field in a spatio-temporal region. The region is divided into subregions called hills and waves which are based on the local form of the surface. They are both three-dimensional tessellations of the spatio-temporal region, and provide an overview of the surface change. To summarize the tessellations, four operations are proposed: section, projection, fusion, and graph representation. They extract useful information from tessellations to describe the structure of surface change. To test the validity of the method, the change of a retail cluster in Shinjuku and Shibuya area in Tokyo is analyzed. The empirical study yields some interesting findings that help us understand changes in the spatial structure of retailing.

## 1. INTRODUCTION

The change of spatial phenomena has drawn much attention of geographers. Residential areas gradually expand with urban growth; retail stores gather around theaters and hotels to form clusters and become shopping malls; people move from small to large cities, which often leads to overconcentration to a few megacities; road networks grow from simple, linear forms to more complicated, web-like forms. These changes have been frequently studied in geography and other related fields.

Analysis of changes, however, was rather impeded by lack of spatio-temporal data in digital format. They were available only in limited cases, and consequently, quantitative analysis in digital environment required manual digitization of time-series maps. The cost of digitization was a major obstacle in spatio-temporal analysis by GIS. Fortunately, this problem is now being solved by the progress of spatial data acquisition tools such as GPS and mobile GIS (Longley *et al*. 1999). The cost of data acquisition is far less expensive today and no longer an impediment to spatio-temporal analysis.

Improvement of data availability can promote spatio-temporal analysis in digital environment. Its methodology, however, is still in the process of development. Most of existing studies perform either spatial or temporal analysis fixing time or location, which is not spatio-temporal analysis in its strict sense (Langran 1992). A summary statistic representing spatial phenomena is calculated at discrete times or time periods and its change is discussed on the temporal axis. Otherwise, a quantitative measure of temporal change is calculated at sample points and its spatial distribution is examined. Though these methods are useful in geographical analysis, there are some cases where they cannot describe the change of spatial phenomena. For example, basic transformations such as translation and rotation are not detectable if we fix time in analysis. This is because spatio-temporality is not explicitly considered. It is obviously desirable to treat changes in their original form, fixing neither space nor time.

This paper proposes a new method for analyzing the change of spatial phenomena, taking its spatio-temporality into consideration. Among various phenomena this paper focuses on the surface, a scalar function defined over a two-dimensional region. Surfaces are used for modelling population distribution (Tobler 1964; Griffith 1981; Bracken 1993; Bracken and Martin 1995), elevation of the earth's surface (Pike 1988; Hutchinson 1989; Etzelmuller 2000), distribution of geological measures (Isaaks and Srivastava 1989; Cressie 1993; Bailey and Gatrell 1995), and so forth. The surface is one of the most important objects in GIS, and its change is of interest to geographers.

To discuss the change of spatial phenomena, we have to consider a spatial region and a time period simultaneously, that is, a spatio-temporal region. In Section 2, we propose two types of tessellations of the spatio-temporal region where a surface function is defined. They are called hills and waves whose definition is based on the local form of the surface. Hills and waves, however, are not easy to analyze directly, because they are both three-dimensional objects. We thus propose four operations to summarize the tessellations in Section 3: section, projection, fusion, and graph representation. These operations help us understand the structure of tessellations, and consequently, the change of the surface. To test the validity of the method, Section 4 analyzes the change of a retail cluster in Shinjuku and Shibuya area in Tokyo, Japan. Section 5 summarizes the conclusions with discussion.

## 2. TESSELLATIONS OF SPATIO-TEMPORAL REGION

The surface is a continuous function defined over a two-dimensional region. Consequently, if it changes over time, it is observed in a three-dimensional region, that is, a spatio-temporal region. This leads to an analysis of the surface in a spatio-temporal region.

To this end, we will propose two types of tessellations of the spatio-temporal region where a surface function is defined. They are used to describe the surface change. Prior to the proposal, however, we first introduce a tessellation of a two-dimensional region, in order to help understanding of the tessellations discussed later.

Suppose a continuous function $f(\mathbf{x})$ defined over a connected region $S$, which is smooth and twice differentiable at any point in $S$ (Figure 1a). Approximating the local surface around every point in $S$ by a quadratic function, we obtain *critical points* where $\frac{\mathrm{d}f(\mathbf{x})}{\mathrm{d}\mathbf{x}} = 0$. Critical points are classified into three categories: peaks, bottoms, and cols (Warntz 1966; Okabe and Masuda 1984). From every point in $S$ an integral curve of the steepest ascent vectors of $f(\mathbf{x})$ runs up to one of the peaks of $f(\mathbf{x})$ (Figure 1b; Warntz 1966; Warntz and Waters 1975; Pfaltz 1976; Okabe and Masuda 1984). This naturally gives a tessellation of $S$ in which each subregion is assigned to one of the peaks of $f(\mathbf{x})$ (Figure 1c).

FIG. 1. A surface and a tessellation of the region. (a) A surface function, (b) peaks (white circles) and integral curves of steepest ascent vectors, (c) a tessellation of the region.

Keeping this tessellation in mind, we proceed to tessellations of the spatio-temporal region. Let $S$ and $T$ be regions defined in the spatial and temporal dimension, respectively. We consider their Cartesian product $S \times T$ and a continuous scalar function $f(\mathbf{x}, t)$ in $S \times T$ which is twice differentiable at any point by both $\mathbf{x}$ and $t$. Differentiating $f(\mathbf{x}, t)$ by $\mathbf{x}$, we obtain a set of critical points discussed above. Since $f(\mathbf{x}, t)$ is a continuous function, they form a finite number of loci in $S \times T$ by which we can trace the movement of critical points. From all the loci we focus on those of peaks, and calculate the tessellation of $S \times T$ as follows. We first fix $t$ at $t_0$, and assign every point in $S$ to one of the peaks to which an integral curve of the steepest ascent vectors of $f(\mathbf{x}, t_0)$ runs up. Moving $t_0$ over $T$, we obtain an assignment of all the points in $S \times T$. We finally reassign every point in $S \times T$ to one of the loci to which its previously assigned peak belongs. Two points in $S \times T$ are assigned to the same locus if they were assigned to peaks in the same locus. This procedure yields a tessellation of the spatio-temporal region $S \times T$ which we call *hills*. In each hill all the points belong to the same locus. Figure 2 shows an example of hills where $S$ is a one-dimensional region.

FIG. 2. Hills (regions bounded by dotted and solid lines) defined by $f(\mathbf{x}, t)$ in $S \times T$, where $S$ is a one-dimensional region.

As shown in Figure 2, hills are bounded by two types of faces. A *Boundary* is a connected set of points that divide $S$ at every $t$ which is depicted as the dotted line in Figures 1 and 2. An *Edge* is another type of face that appears with generation and disappearance of hills (solid lines in Figure 2). When a hill disappears, a set of points around the peak are suddenly reassigned to another hill. This yields a face perpendicular to the temporal axis.

Hills represent the history of two-dimensional subregions shown in Figure 1c. Generation and disappearance of a subregion is indicated by edges of hills. Boundaries tell us how the tessellation changes over time. Section of hills at a time gives their snapshot as a two-dimensional tessellation.

Hills are three-dimensional objects in the spatio-temporal region, though they are illustrated as two-dimensional in Figure 2. Similarly, both boundaries and edges are two-dimensional objects. Consequently, hills and their boundaries do not always have simple shapes; a hill may have another hill inside itself.

Interchanging $S$ and $T$ in the above discussion, we obtain another tessellation of the spatio-temporal region $S \times T$. Differentiating $f(\mathbf{x}, t)$ by $t$, we obtain a set of temporal peaks of $f(\mathbf{x}, \mathrm{t})$ where $\frac{\partial f}{\partial t} = 0$ and $\frac{\partial^2 f}{\partial t^2} < 0$. Temporal peaks, as well as spatial peaks, form a finite number of connected faces in $S \times T$. Fixing $\mathbf{x}$ at $\mathbf{x}_0$, we assign every point in $T$ to one of the temporal peaks by climbing up the steepest ascent vectors of $f(\mathbf{x}_0, t)$, which yields a tessellation of the one-dimensional region $T$ (Figure 3). Therefore, reassignment of points to the faces to which the peaks belong yields a tessellation of $S \times T$ by the faces, the set of temporal peaks. We call the tessellation *waves* (Figure 4).

FIG. 3. Tessellation of the one-dimensional region $T$. (a) The section of $f(\mathbf{x}, t)$ at $\mathbf{x}=\mathbf{x}_0$, (b) tessellation of $T$ at $\mathbf{x}_0$ by $f(\mathbf{x}_0, t)$.

FIG. 4. Waves defined by $f(\mathbf{x}, t)$ in $S \times T$, where $S$ is a one-dimensional region.

Waves have also two types of faces as shown in Figure 4. A connected set of points dividing $T$ at every $\mathbf{x}$ is called a *boundary* (dotted lines in Figure 3 and 4); to distinguish it from that of hills, we may say a *wave boundary*. The other is called an *edge* or a *wave edge*, which appears at the spatial margin of waves. The wave edge is a concept corresponding to the hill edge.

A wave is a connected set of points in $S \times T$ that share the change pattern of $f(\mathbf{x}, t)$. A set of locations $S_0$ belong to the same wave for a limited time period $T_0$ if $f(\mathbf{x}, t)$ in $S_0$ changes similarly during $T_0$. Let us consider, for example, spatial distribution of rent in a business district. When business is going well, rent rises everywhere in the district. In depression phase, however, rent gradually goes down. Though there is a slight time lag among locations, the business district shares the change pattern of rent. Therefore, the district belongs to the same wave during the cycle of business.

Hills and waves are dual concepts of tessellations in the spatio-temporal dimension. Consequently, they have many similarities such as boundaries and waves. However, the difference of dimension between space and time causes several differences between them. For example, the generator of a hill is a one-dimensional object, that is, a locus of spatial peaks. On the other hand, a wave is assigned to a two-dimensional object - a face consisting of temporal peaks. Because of this, only waves can be divided further into small pieces - former and latter halves, which often have an important meaning as shown in Section 4. In addition, waves can be arranged by their order on the temporal axis; waves compose a semiordered set.

## 3. SUMMARY REPRESENTATION OF TESSELLATIONS

Hills and waves proposed in the previous section are both three-dimensional objects in the spatio-temporal region. Unfortunately, it is not easy at present to analyze three-dimensional objects directly because of the following reasons: 1) it is difficult to visualize them in a three-dimensional space; 2) compared to two-dimensional objects, three-dimensional objects convey a great amount of information; 3) GIS is not yet able to deal with three-dimensional objects in vector format. To avoid these difficulties, we propose several methods for summarizing tessellations which help us understand their structure.

*3.1 Section*

A simple but useful method to analyze three-dimensional objects is to make their sections by planes and lines. Fixing time *t*, we can visualize the structure of tessellations on a plane. The section by line is usually made along the temporal axis at a fixed location. If we add identification numbers to hills and waves, we can trace the surface change, say, the movement of hills, on a set of sections. Sections are effective at an early stage of analysis, especially in exploratory spatio-temporal analysis.

*3.2 Projection*

A more sophisticated method of summarization is to make projections of tessellations on *S* and *T*. A projection of hill boundaries on *S* indicates the extent of their movement. A projection of hill edges on *T* shows the frequency distribution of generation and disappearance of hills.

Let us consider, for example, the projection of hill boundaries *B* on *S*. Let $1_B(\mathbf{x}, t)$ be the indicator function of boundaries, that is,

$$1_B(\mathbf{x},t)=\begin{cases}1 & \text{if a boundary exists at } (\mathbf{x},t)\\ 0 & \text{otherwise}\end{cases}. \tag{1}$$

An ordinary projection of *B* on *S* is given by

$$P_0(\mathbf{x},B;S)=\begin{cases}1 & \text{if } \exists t\in T, 1_B(\mathbf{x},t)\neq 0\\ 0 & \text{otherwise}\end{cases}. \tag{2}$$

This projection represents the shadow of boundaries by the light parallel to the temporal axis. This definition, however, is not useful if hills are so small that there are many boundaries in $S\times T$; the function $P_0(\mathbf{x}, B; S)$ is equal to one almost everywhere.

To avoid this problem, we slightly modify the definition of projection operation: objects are smoothed by a distance-decay weighting function in projection. The projection of hill boundaries is then mathematically defined by

$$P(\mathbf{x},B;S)=\int_{t\in T}\int_{\mathbf{y}\in S}1_B(\mathbf{y},t)w(|\mathbf{x}-\mathbf{y}|)\mathrm{d}\mathbf{y}\mathrm{d}t, \tag{3}$$

where $w(r)$ is a weighting function. One example of the weighting function is a Gaussian function

$$w(r)=\exp\left[-\left(\frac{r}{R}\right)^2\right]. \tag{4}$$

The projection of boundaries on *T* is given by

$$P(t,B;T)=\int_{\mathbf{x}\in S}\int_{u\in T}1_B(\mathbf{x},u)w'(|t-u|)\mathrm{d}u\mathrm{d}\mathbf{x}, \tag{5}$$

where $w'(r)$ is a weighting function. Projections of edges can also be made in a similar way.

Projections on $S$ represent spatial stability of hills and waves. If hills do not change their shape and location in $T$, the boundaries give dark shade in their projection, and consequently, $P(\mathbf{x}, B; S)$ shows a wild fluctuation. Dark shade of wave edges indicates that waves occur at the same location.

Projections on $T$, on the other hand, reflect the distribution of topological events - generation and disappearance of hills and waves. Concentration of topological events makes the projection partially dark. If topological events are uniformly distributed in $T$, the projection shows a uniform light shade.

*3.3 Fusion*

The above two methods reduce the amount of information conveyed by tessellations. These methods, however, do not necessarily keep important and useful information about the surface change; it is difficult to make appropriate sections of tessellations before understanding their structure. One method to assure that is to use fusion operation, that is, to combine small hills and waves into larger ones. This is based on the assumption that larger hills and waves are more important than smaller ones in analysis of surface changes.

In fusion operation, evaluation of the size of hills and waves is critical. A simple but reasonable measure is their volume which is defined as follows. Let $H_i$ be the $i$th hill in $S \times T$, whose indicator function is given by

$$1_{H_i}(\mathbf{x},t) = \begin{cases} 1 & \text{if } (\mathbf{x},t) \in H_i \\ 0 & \text{otherwise} \end{cases}. \tag{6}$$

The volume of $H_i$ is defined by

$$vol(H_i) = \int_{t \in T} \int_{\mathbf{x} \in S} 1_{H_i}(\mathbf{x},t) \mathrm{d}\mathbf{x} \mathrm{d}t. \tag{7}$$

Hills whose volume is less than a certain value are regarded as insignificant and combined into neighboring hills.

In some applications, the surface height is also important. To take it into account, we can use the height of $H_i$ defined by

$$height(H_i) = \max_{\mathbf{x} \in H_i} f(\mathbf{x},t) - \min_{\mathbf{x} \in H_i} f(\mathbf{x},t), \tag{8}$$

its absolute intensity

$$int(H_i) = \int_{t \in T} \int_{\mathbf{x} \in S} f(\mathbf{x},t) 1_{H_i}(\mathbf{x},t) \mathrm{d}\mathbf{x} \mathrm{d}t, \tag{9}$$

and its relative intensity

$$int(H_i) = \int_{t \in T} \int_{\mathbf{x} \in S} \left\{ f(\mathbf{x},t) - \min_{\mathbf{x} \in H_i} f(\mathbf{x},t) \right\} 1_{H_i}(\mathbf{x},t) \mathrm{d}\mathbf{x} \mathrm{d}t. \tag{10}$$

In addition to the above, there are several measures useful for distinguishing significant hills from insignificant ones: the area of projection of hills on $S$, the length of projection of hills on $T$, and so forth. The choice of the measure depends on the objective of analysis.

Hills and waves judged to be small and insignificant are combined into larger ones. There is a choice of hills into which small hills are combined. One reasonable choice is the largest hill among neighboring ones. This method is used to eliminate spurious polygons in GIS (Star and Estes 1990). If the surface height is important, we combine a small hill into the neighboring one that gives the smallest relative depth of boundaries (Figure 5). This approach is often taken in topological analysis of surfaces and temporal functions (Okabe and Masuda 1984; Sadahiro 2000; Okabe and Masuyama 2001).

FIG. 5. Merging a small hill into larger one. $H_1$, $H_2$, $H_3$: hills, $B_2$, $B_3$: boundaries. (a) Relative depth of boundaries with respect to the hill $H_1$, (b) $H_1$ is combined into $H_2$ because the boundary $B_2$ is shallower than $B_3$.

*3.4 Graph representation*

If the topological structure of tessellations is of interest, graph representation of hills and waves works effectively in analysis. Hills and waves are represented by nodes, while boundaries and edges by links. For example, waves shown in Figure 2 are represented by the graph in Figure 6.

FIG. 6. Graph representing the topological structure of waves shown in Figure 2. Waves are represented as nodes, while boundaries and edges by links.

Graphs are useful for not only description of the global structure of tessellations but also comparison of tessellations. Let us consider two spatio-temporal regions in both of which surface functions are defined. We say that the surface changes are topologically equivalent if the graphs representing hills and waves are isomorphic between the regions. We can also evaluate the difference between surface changes by a distance measure defined for comparison of graphs.

*3.5 Combination of several methods*

The methods proposed above can be used not only separately but also together in analysis. Suppose that we are interested in the spatial structure of significant hills. To remove insignificant hills, we apply the fusion operation to combine small hills into larger ones. We then describe the topology of hills by a graph, and may finally make a projection of the graph on $S$. If we are interested in the stability of hill boundaries, we again remove insignificant hills by fusion operation and make a projection of hill boundaries on $S$. Combination of several methods extends applicability of hills and waves.

## 4. EMPIRICAL STUDY

This section empirically analyzes the change of a surface in order to test the validity of the method proposed in Sections 2 and 3. We investigate the change of retail activity in Shinjuku and Shibuya area in Tokyo, Japan (Figure 7). The study region has the biggest retail cluster in Japan, surrounded by urban parks, residential areas and business districts. The Yamanote Line and Meiji Street run through the region, and there are five major railway stations: Shinjuku, Yoyogi, Harajuku, Shibuya, and Ebisu.

FIG. 7. Shinjuku and Shibuya area in Tokyo, Japan.

Spatial data used in the analysis are based on the list of retail stores and restaurants in the *NTT telephone directory* which is published monthly. We extracted their addresses in September every year from 1990 to 99 in ASCII format, and converted them into point data by geocoding. Figure 8 shows the number of retail stores and restaurants in the study region from 1990 to 99.

FIG. 8. The number of retail stores and restaurants, 1990-99.

From the point data we calculated the density distribution of stores at time $i$ ($i$=1990, 91, ..., 99) using

$$f(\mathbf{x},t_i)=\sum_j \exp\left[-\left(\frac{\left|\mathbf{x}-\mathbf{y}_{ij}\right|}{R}\right)^2\right], \tag{11}$$

where $\mathbf{y}_{ij}$ is the locational vector of store $j$ at time $i$ and $R$ is the distance decay parameter. We tried three values for $R$, 100m, 150m, and 200m, but show only the result of $R$=150m due to the limitation of space. From the set of density distributions we estimated the surface change from 1990 to 99 by linear interpolation at lattice points of resolution 10m.

Figure 9 shows the density distributions of stores in 1990 and 99. There were two big subclusters in the study region, one at the northeast of Shinjuku, and the other at the west of Shibuya. In addition, there were smaller subclusters at the east and west of Shinjuku, the east of Harajuku and the southwest of Ebisu. These subclusters existed in both 1990 and 1999, which implies the global stability of retail activity in the region.

FIG. 9. Density distribution functions of retail stores and restaurants, 1990 and 99.

We then calculated the tessellations of the region, 1990-99. To eliminate insignificant hills, we performed fusion operation to combine hills whose relative height is less than 150 into the highest neighboring hills. As a result, we obtained 90 hills and 83 waves.

Figure 10 shows the distribution of absolute intensity of hills and waves defined by equation (9). Intensity of hills decreases linearly with the rank, while that of waves has an S-shaped figure. This indicates that the intensity of waves has larger variance than that of hills.

FIG. 10. Hills and waves arranged in order of the intensity.

Figure 11 shows the sections of hills in 1990 and 99, including the graphs representing the topological structure of hills. There were 22 hills in 1990 along Yamanote Line; there were several hills that cannot be recognized in Figure 9. Comparing the figures we notice that two hills disappeared and three were newly generated since 1990. The topology of hills represented by links had also changed, especially around Shinjuku and Ebisu stations.

FIG. 11. Sections of hills and their graph representation, 1990 and 99.

Figure 11 suggests that the spatial structure of retailing had slightly changed at the local scale. To analyze the change in more detail, we extracted stable hills that had existed throughout the period; other hills were combined into neighboring ones by fusion operation. Average and standard deviation of lifetime of hills are 4.19 and 3.18 years, respectively.

Figure 12 shows the topology of stable hills. The figure indicates, against our expectation, that the surface had considerably changed its spatial structure. There are only 11 stable hills, half of the hills that existed in 1990. They are recognizable in Figure 9, that is, relatively large hills. From this we conclude that the spatial structure of retailing was stable at the global scale while it had drastically changed at the local scale.

FIG. 12. Stable hills and their topology.

In the above discussion we have focused on the topological structure of hills and its stability over time. We then move to the stability of hills and waves with respect to the absolute location in the spatio-temporal region. To this end, boundaries and edges of hills and waves were projected on $S$ and $T$. In calculation of the projections, hills and waves were weighted by the sectional intensity whose definition for hill boundaries is given by

$$int_S(H_i,t)=\int_{\mathbf{x}\in S}\left\{f(\mathbf{x},t)-\min_{\mathbf{x}\in H_i} f(\mathbf{x},t)\right\}1_{H_i}(\mathbf{x},t)\mathrm{d}\mathbf{x}. \tag{12}$$

The projection of hill boundaries is then

$$P_S(\mathbf{x},B;S)=\int_{t\in T}\sum_i int_S(H_i,t)\int_{\mathbf{y}\in S}1_{B_i}(\mathbf{y},t)w(|\mathbf{x}-\mathbf{y}|)\mathrm{d}\mathbf{y}\mathrm{d}t, \tag{13}$$

where $1_{Bi}(\mathbf{x}, t)$ is the indicator function of the $i$th boundary. Figures 13 and 14 show the projections on $S$ and $T$, respectively.

FIG. 13. The projections of hill boundaries and wave edges on $S$. (a) Hill boundaries, (b) wave edges.

FIG. 14. The projections of hill edges and wave boundaries on $T$. (a) Hill edges, (b) wve boundaries.

In Figure 13a we notice that the projection of hill boundaries clearly reflects the surface distributions in 1990 and 99 shown in Figures 9 and 11. This supports our earlier observation - global stability of retail activity in the region. In the south of the study region, however, the projection shows relatively small values. The spatial structure of retailing is rather unstable in that region.

Let us compare the projections of hill boundaries and wave edges on $S$ in Figure 13. If they have similar shapes, it means that changes occur within hill boundaries; correlation between spatial patterns of the surface and its temporal change. If they are different, surface changes involve several hills. Concerning Figures 13a and 13b, we should say that they are partly similar. In the north of the study region, both boundaries and edges run from the west to the north east of Shinjuku station; linear pattern appears to the south of Yoyogi station in both figures. Changes of the surface are restricted by its spatial structure - they usually occur within hill boundaries. In the south, on the other hand, boundaries and edges have quite different, even reverse patterns; most boundaries run from southwest to northeast, while edges run from southeast to northwest. There is little spatio-temporal correlation in the surface change in that region.

Let us turn to Figure 14. The figures are quite similar; hill edges and wave boundaries had both gradually increased from 1990, reached the peak in 1995, and decreased thereafter. The peak of hill edges in 1995 indicates drastic generation and disappearance of hills, that is, great changes in the spatial structure of retailing. The projection of wave boundaries, on the other hand, should be discussed in relation to the number of retail stores and restaurants shown in Figure 8. Stores had continuously decreased from 1990 to 1995, and gradually increased until 1998. This caused disappearance of old waves and generation of new waves in 1995. From these observations, we say that the spatial structure of retailing drastically changes when the number of stores reaches the bottom - when the retail activity is in depression.

Generation and disappearance of hills are significant changes in the spatial structure of retailing. One clue to understand these phenomena is, as shown above, that they occur when the retail activity is in depression. To analyze it in more detail, we examine the location of hill generations in relation to the size of waves. From 1990 to 99, there are 24 generations of hills which are concentrated in the 10 largest waves out of 83. Since the generation seems likely to occur in large waves, we performed the binomial test to examine whether the hill generation occurs more frequently in larger waves. The null hypothesis of random distribution was rejected at the significance level 1%, which supports our hypothesis. Hills are generated by large waves, not by small waves. Since the same result was obtained for the disappearance of hills, we conclude that the spatial structure of retailing is more likely to change by large, long-term trends. In other words, small and short-term trends are not enough to change the spatial structure of retailing.

We finally test whether the generation and disappearance of hills occur more frequently in the former half of waves rather than their latter half (recall Section 2). The binomial test, however, did not reject the null hypothesis of complete randomness. The distribution of generation and disappearance is not biased with respect to the temporal peaks of waves.

## 5. CONCLUSION

In this paper we have developed a method for analyzing surface changes by tessellations. The change of a surface is represented by a scalar field in a spatio-temporal region. The spatio-temporal region is divided into hills and waves whose definition is based on the local form of the surface. They are both three-dimensional objects representing the spatio-temporal structure of the surface change. Unfortunately, hills and waves are not easy to analyze directly because of the difficulty in visualization and understanding of a great amount of information they convey. We thus proposed four operations to summarize the tessellations: section, projection, fusion, and graph representation. They extract useful information from the tessellations to describe the structure of surface change. To test the validity of the method, we analyzed the change of a retail cluster in Shinjuku and Shibuya area in Tokyo, Japan. The empirical study yielded some interesting findings that help us understand the change of the spatial structure of retailing.

In geographical analysis, visual analysis plays an important role not only at an early stage of analysis but also in mathematical modelling. Hills and waves, however, are difficult to visualize as three-dimensional objects though they give us a great amount of information about the structure of surface change. Consequently, visualization of hills and waves is inevitably accompanied by dimension reduction, some of which are described in Section 3. The choice of the reduction method heavily depends on the objective of analysis. Users should carefully choose an appropriate method taking their objective into account.

The empirical study shown in Section 4 is at an early stage as location analysis: we treated all the stores and restaurants equally, neglecting their category, size, customers, and so forth. This is because we are interested in the spatial aspect of retailing rather than its attribute distribution and spatial correlation between them. However, the study can be further extended to take more factors into account in analysis. For example, the density distributions of stores and the tessellations of the region are both obtained from the point data of stores and restaurants. Therefore, hills and waves inherit the attributes of their original points, and their spatial structures can be analyzed in relation to their non-spatial properties by multivariate statistical methods including spatial autocorrelation coefficients. Another way to treat diversity in stores and restaurants is to classify them by their attributes and calculate surfaces for individual categories. Comparison of tessellations would reveal the difference and relationship among surface changes, typical patterns of the surface change, and so forth.

We finally discuss some limitations of our method for further research. First, surfaces are usually estimated from a set of data measured at sample points. To convert the discrete data into continuous form, we perform spatial interpolation such as spline (Spath 1995), kriging (Isaak and Srivastava 1989; Cressie 1993), and kernel estimation (Silverman 1986; Scott 1992). In addition, as done in the empirical analysis, the surface change is estimated from a set of surfaces of different times by temporal interpolation. This implies that hills and waves calculated from the real data depend on the interpolation method. One practical solution to this problem is to use fusion operation to eliminate small hills and waves which are relatively unstable against the change of interpolation methods. We can greatly reduce arbitrariness in the results of analysis by focusing only on significant hills and waves. Another method to avoid the difficulty is to acquire spatial data at a high resolution in both spatial and temporal dimensions. This is now a feasible option because we have various tools for spatial data acquisition as discussed in the introductory section. However, the ultimate solution is to develop spatio-temporal interpolation techniques suitable for analysis of surface changes (Sadahiro 2000). New methods that explicitly take the behavior of surfaces into account should be developed in future research. Second, hills and waves give tessellations of the spatio-temporal region which are based the first derivative of the surface function. In some applications, however, it may be necessary to discuss more detailed topography of surfaces, say, aspect of slopes, ridge and course lines, and other concepts calculated from higher order derivatives of the surface. Improvement of the ability of representing surfaces is an important subject for future research.

**LITERATURE CITED**

Bailey, T. C. and A. C. Gatrell (1995). *Interactive Spatial Data Analysis*. London: Taylor & Francis.

Bracken, I. (1993). "An Extensive Surface Model Database for Population-Related Information." *Environment and Planning B* **20**, 13-27.

Bracken, I. and D. Martin (1995). "Linkage of the 1981 and 1991 UK Censuses Using Surface Modelling Concepts." *Environment and Planning A* **27**, 379-390.

Cressie, N. (1993). *Statistics for Spatial Data*. New York: John Wiley.

Etzelmuller, B. (2000). "On the Quantification of Surface Changes using Grid-based Digital Elevation Models (DEMs)." *Transactions in GIS* **4**, 129-143.

Griffith, D. A. (1981). "Modeling Urban Population Density in a Multicentered City." *Journal of Urban Economics* **9**, 298-310.

Hutchinson, N. F. (1989). "A New Procedure for Gridding Elevation and Stream Line Data with Automatic Removal of Spurious Pits." *Journal of Hydrology* **106**, 211-232.

Isaaks, E. H. and R. M. Srivastava (1989). *An Introduction to Applied Geostatistics*. New York: Oxford University Press.

Langran, G. (1992). *Time in Geographic Information Systems*. London: Taylor & Francis.

Longley, A., M F. Goodchild and D. J. Maguire, D. J. (1999). *Geographic Information Systems: Principles, Techniques, Applications and Management*. New York: John Wiley.

Okabe, A. and S. Masuda (1984). "Qualitative Analysis of Two-dimensional Urban Population Distribution in Japan." *Geographical Analysis* **16**, 301-312.

Okabe, A. and A. Masuyama (2001). "An Exploratory Method for Qualitative Trend Curve Analysis - A Robust Method against Low Quality Data." *International Journal of Geographical Information Science*, to appear.

Pike, R. J. (1988). "The Geometric Signature: Quantifying Landslide-Terrain Types from Digital Elevation Models." *Mathematical Geology* **20**, 491-511.

Pfaltz, J. L. (1976). "Surface Networks." *Geographical Analysis* **8**, 77-93.

Sadahiro, Y. (2000). "Event-Based Analysis of Changes in Surfaces." *CSIS Discussion Paper Series* **31**, Center for Spatial Information Science, University of Tokyo, Japan (http://www.csis.u-tokyo.ac.jp/dp/31.pdf).

Scott, D. W. (1992). *Multivariate Density Estimation*. New York: John Wiley & Sons.

Silverman, B. W. (1986). *Density Estimation*. London: Chapman & Hall.

Spath, H. (1995). *Two Dimensional Spline Interpolation Algorithm*. Wellesley, MA: A K Peters.

Star, J. and J. Estes (1990). *Geographic Information Systems: An Introduction*. Englewood Cliffs, NJ: Prentice-Hall.

Tobler, W. (1964). "A Polynomial Representation of the Michigan Population." *Papers of the Michigan Academy of Science, Arts, and Letters* **49**, 445-452.

Warntz, W. (1966). "The Topology of a Socioeconomic Terrain and Spatial Flows." *Papers of the Regional Science Association* **17**, 47-61.

Warntz, W. and N. Waters (1975). "Network Representations of Critical Elements of Pressure Surface." *Geographical Review* **65**, 476-492.

(a) (b) (c)

Figure 1

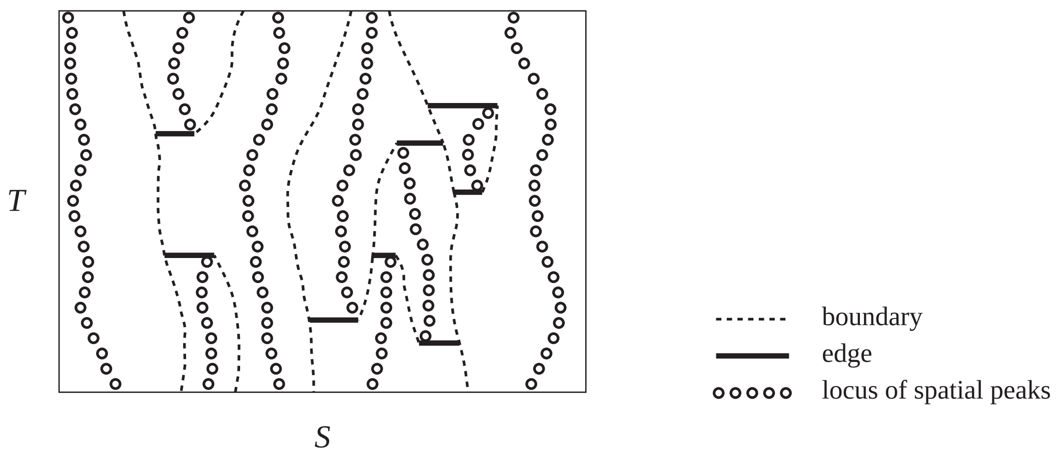


Figure 2

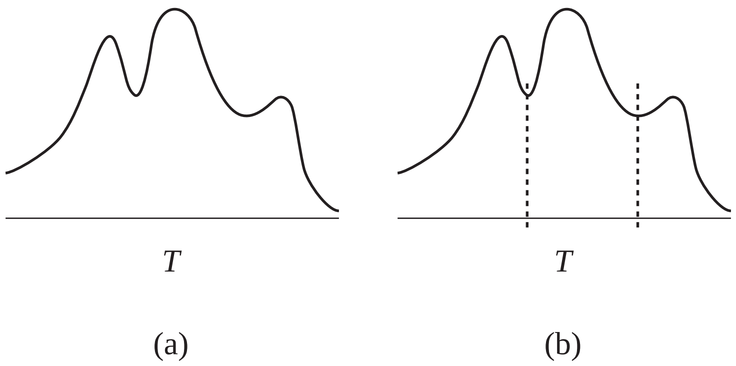


Figure 3

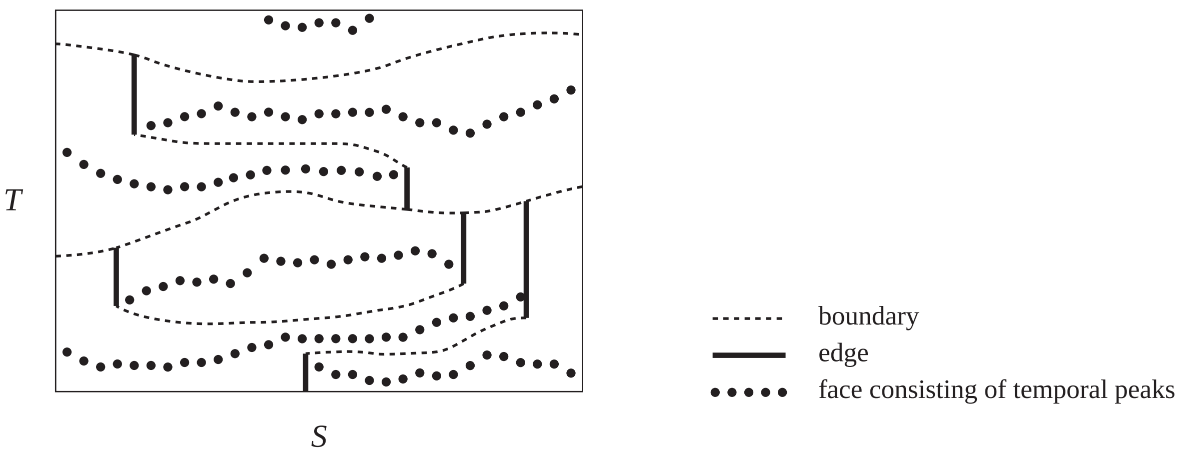


Figure 4

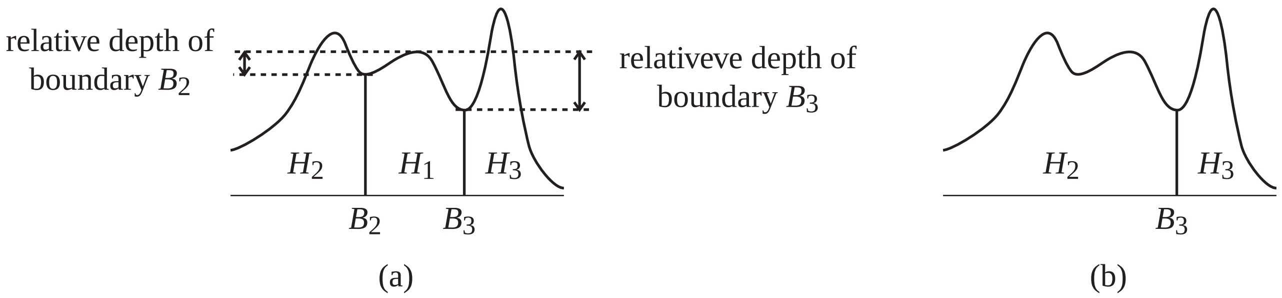
relative depth of
boundary $B_2$
$H_2$
$H_1$
$H_3$
$B_2$
$B_3$
(a)
relativeve depth of
boundary $B_3$
$H_2$
$H_3$
$B_3$
(b)

Figure 5

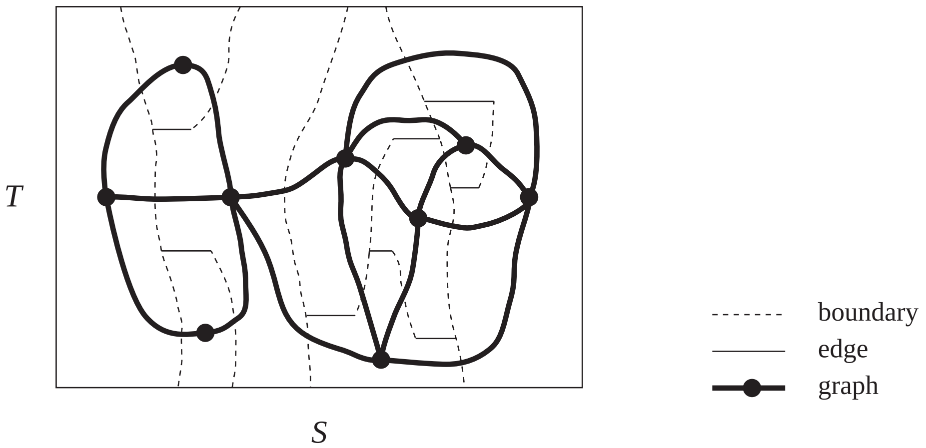


Figure 6


Shinjuku
Yoyogi
Yamanote
Line
Meiji
Street
Harajuku
Shibuya
Ebisu
railway
Yamanote Line
railway
Meiji Street
study region
urban parks

Figure 7

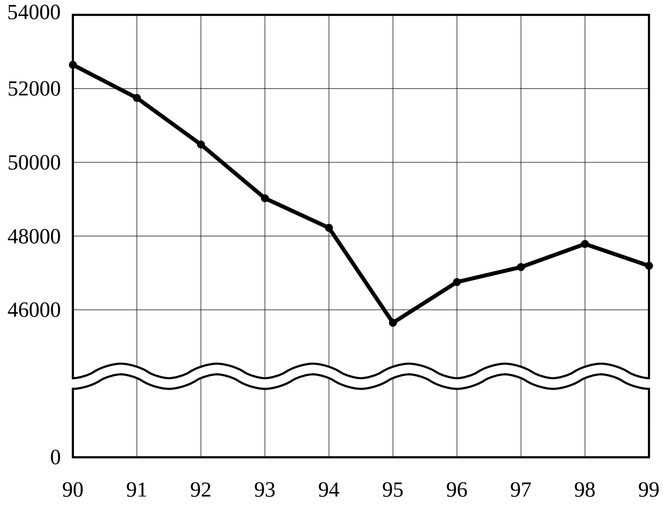


Figure 8

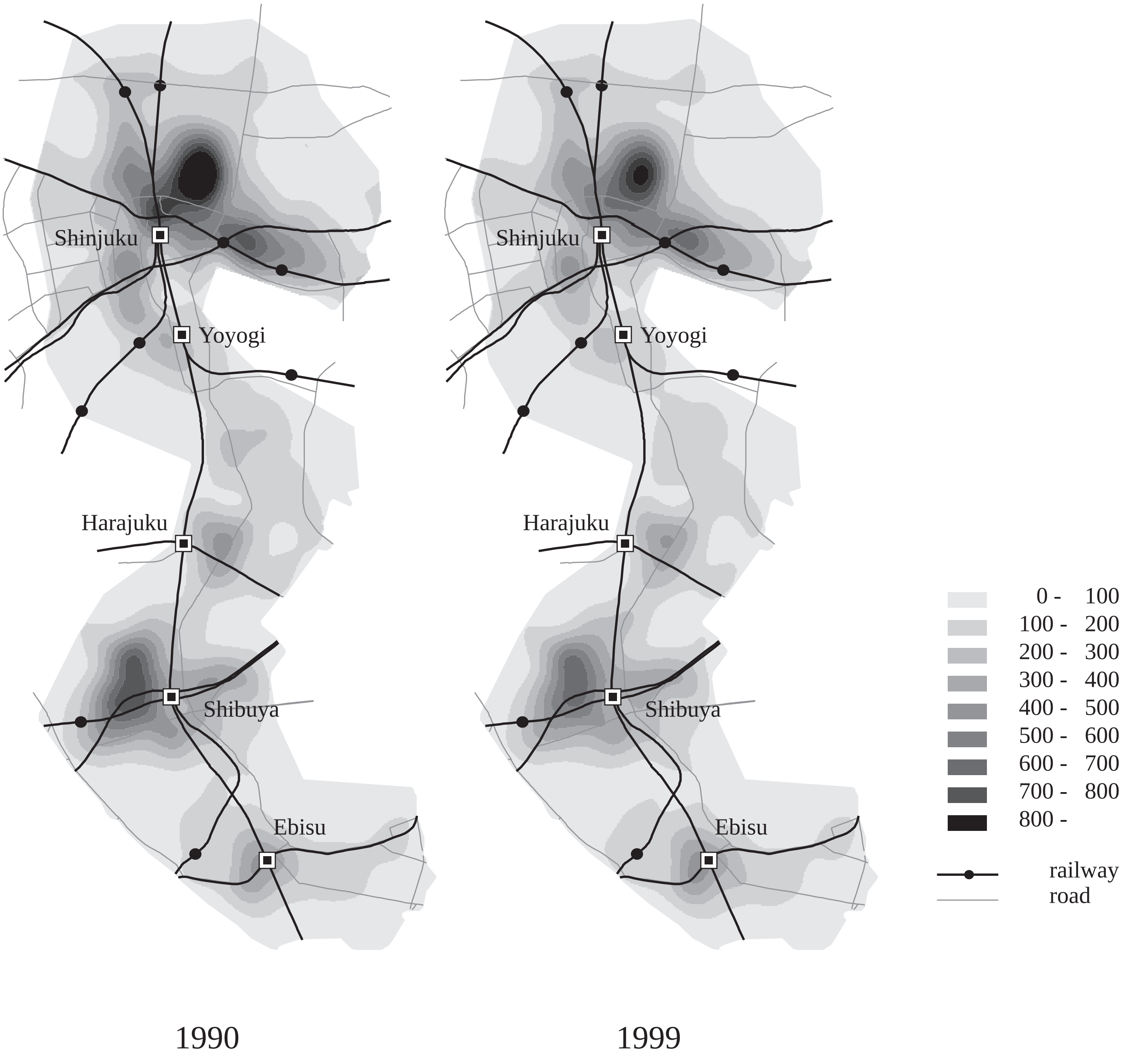
Shinjuku
Yoyogi
Harajuku
Shibuya
Ebisu
1990
Shinjuku
Yoyogi
Harajuku
Shibuya
Ebisu
1999
0 - 100
100 - 200
200 - 300
300 - 400
400 - 500
500 - 600
600 - 700
700 - 800
800 -
railway
road

Figure 9

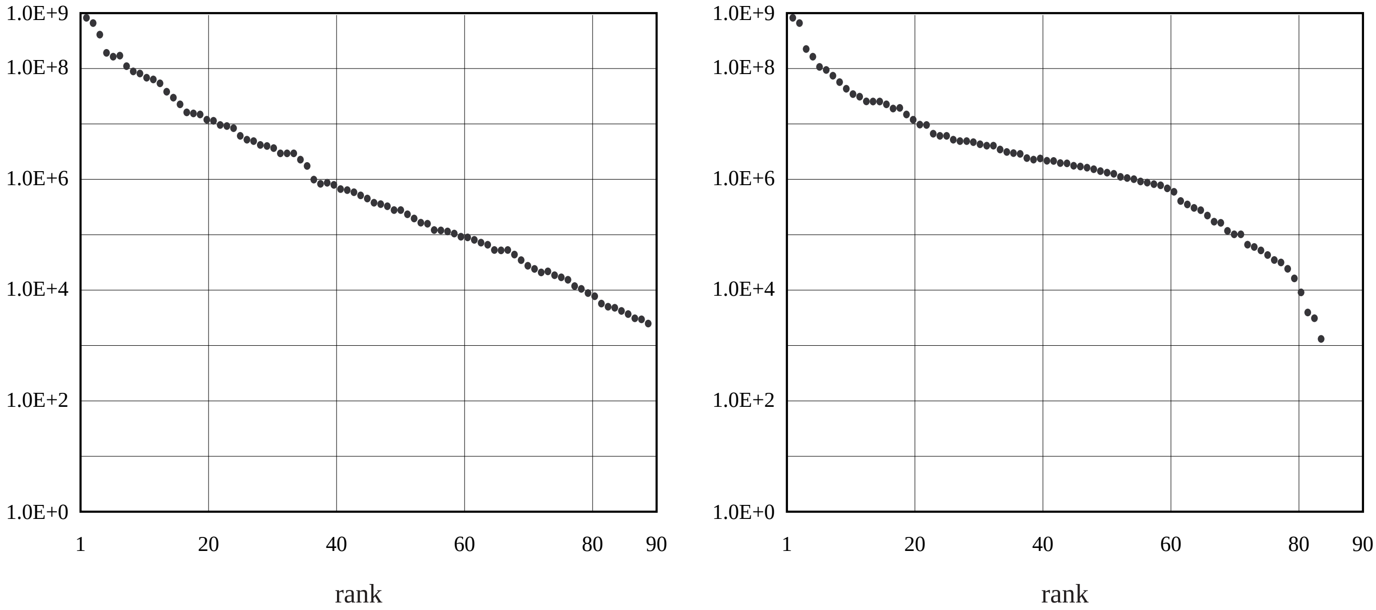


intensity of hills

intensity of waves

Figure 10


# Figure 11

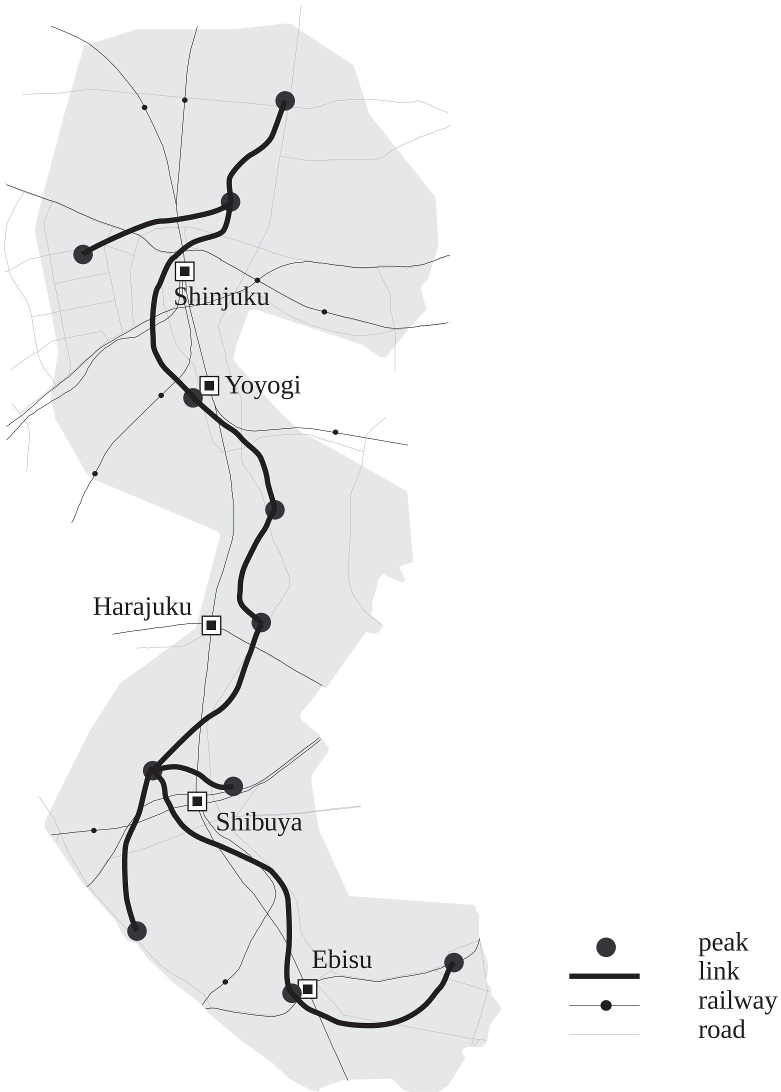
Shinjuku
Yoyogi
Harajuku
Shibuya
Ebisu
peak
link
railway
road

Figure 12

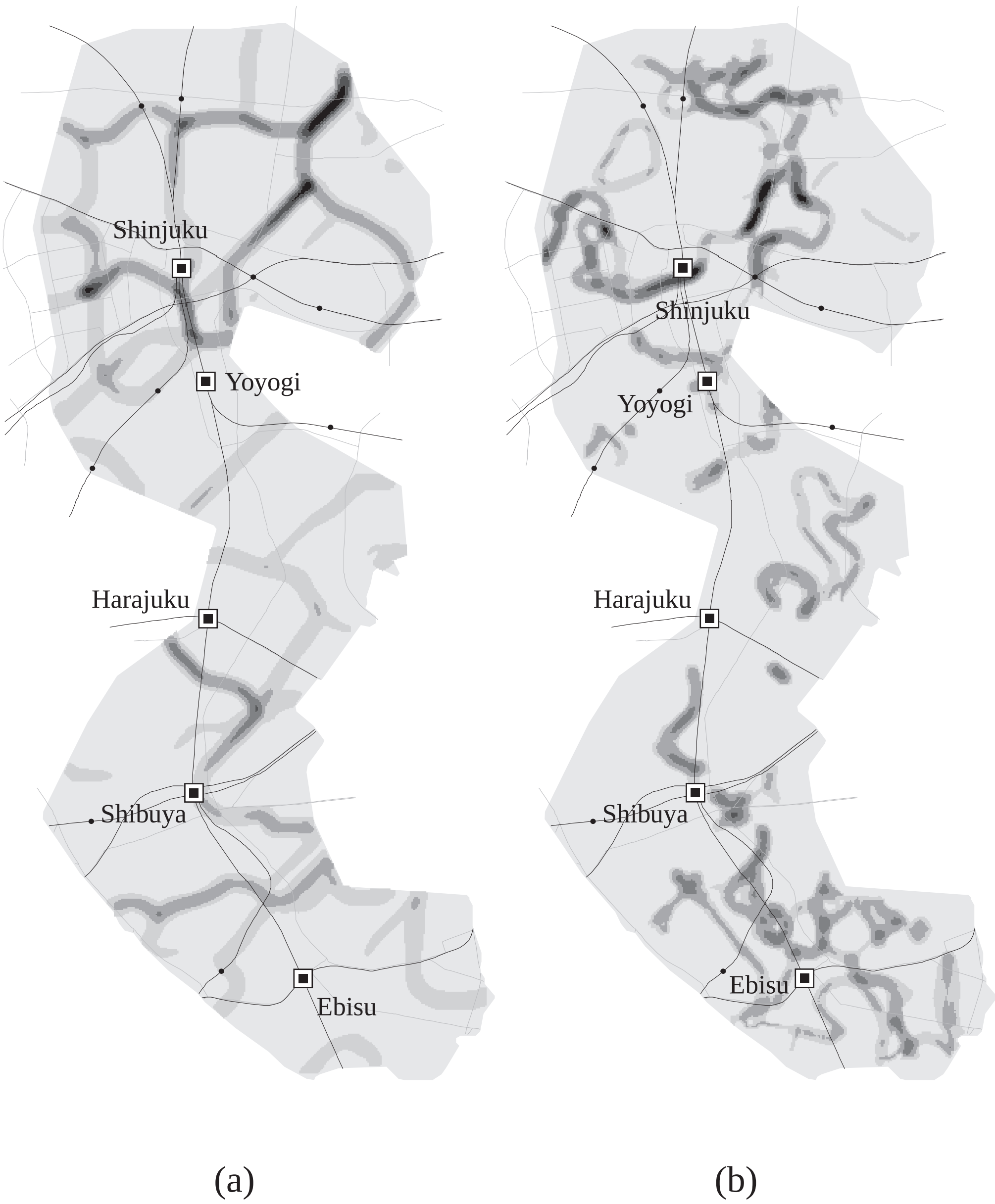
Shinjuku
Yoyogi
Harajuku
Shibuya
Ebisu
(a)
Shinjuku
Yoyogi
Harajuku
Shibuya
Ebisu
(b)

Figure 13

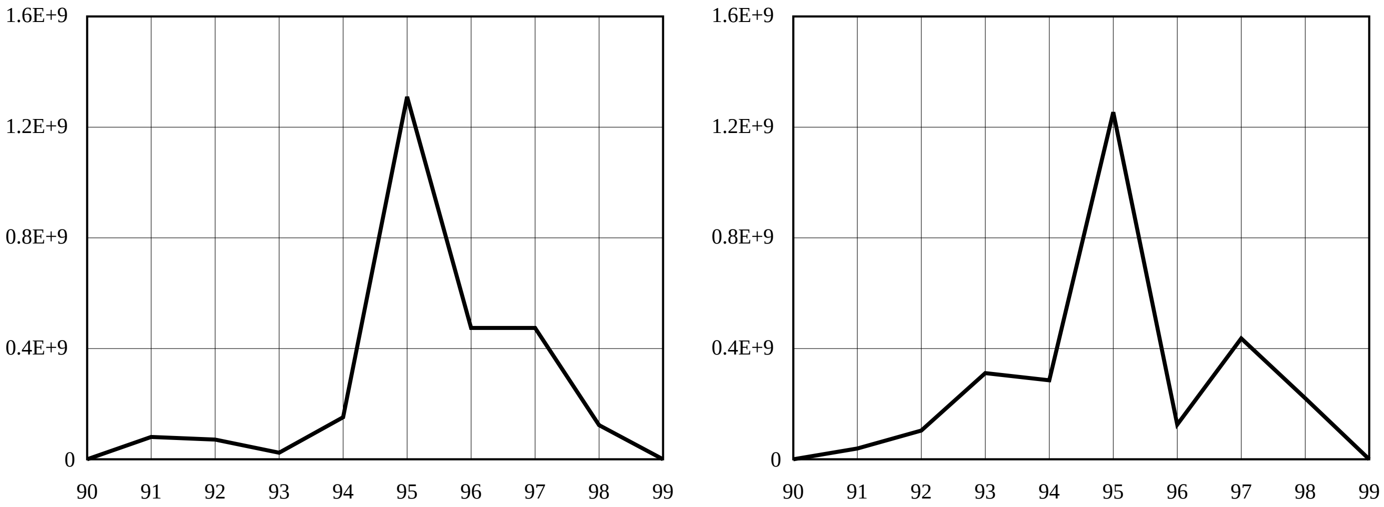


(a)

(b)

Figure 14